Effect of Addition of Polyoxypropylenediamine on the Morphology and Mechanical Properties of Maleated Polypropylene/Maleated Rubber Blends

TAM THI MINH PHAN,[1] ANTHONY J. DENICOLA, JR.,[1] LINDA S. SCHADLER[2]

[1] Montell Polyolefins, R&D Center, Elkton, Maryland 21921

[2] Rensselaer Polytechnic Institute, Troy, New York 12180-3590

Received 14 March 1997; accepted 12 October 1997

ABSTRACT: Blends of maleated polypropylene and maleated ethylene propylenediene (EPDM-*g*-MA) were compounded in a twin-screw extruder with a polyetheramine (PEA), polyoxypropylenediamine, as a compatibilizer. The effect of the compatibilizer concentration and molecular weight on the physical properties was investigated. FTIR data showed that the addition of the compatibilizer caused an imide linkage to form between the amine functionality on the PEA and the maleic anhydride (MA) functionality on both the polypropylene (PP) and the rubber backbone. This bond improved the interfacial adhesion between the rubber and the PP matrix, resulting in an improvement in the toughness of the blends. Other improvements in the physical properties of the blends with a compatibilizer compared to the blends without it included notched Izod impact, elongation at yield, and elongation at break. The optimum improvement in properties was found when the level of the compatibilizer was about 3 wt %. These changes in properties correlated well with the morphology observed via optical and scanning electron microscopy. © 1998 John Wiley & Sons, Inc. J Appl Polym Sci 68: 1451–1472, 1998

INTRODUCTION

Polypropylene (PP) is one of the most versatile commodity polymers because it possesses exceptional properties including excellent chemical and moisture resistance, good ductility and stiffness, and low density. It is also easy to process and relatively inexpensive. It is well known, however, that the good properties of isotatic PP as an engineering polymer matrix are seriously limited by the lack of impact resistance and the inability of this polymer to create a high-level interfacial adhesion to the surface of other phases such as rubber, ceramic fillers, or other polar materials like urethanes, epoxies, or melamines. This is primarily due to the nonpolar nature of PP.[1]

To improve the impact resistance of the PP matrix, rubbers have been used as impact modifiers. Extensive research has been published on blends of polypropylene with ethylene–propylene rubber (PP/EPR), polypropylene with the ethylene–propylenediene monomer (PP/EPDM),[2–8] polypropylene with the styrene–ethylene butylene–styrene triblock copolymer (PP/SEBS),[9,10] and polypropylene with natural rubber (PP/NR).[11–13] Interest has centered primarily on the use of EPR or EPDM rubbers because these blends have the best balance between properties and cost. Although the PP and rubber structures are similar, PP/rubber blends are immiscible with poor interfacial adhesion between the rubber and the PP matrix.[1,2,5,7,14] The two components can be solution-blended at the molecular level, but phase sep-

Correspondence to: T. T. M. Phan.
Contract grant sponsor: Montell Polyolefins.

Journal of Applied Polymer Science, Vol. 68, 1451–1472 (1998)
© 1998 John Wiley & Sons, Inc. CCC 0021-8995/98/091451-22

aration persists.[15] This limits the mechanical properties. To improve the mechanical properties of the final blends, attempts have been made to enhance the miscibility and/or the polymer/rubber interfacial interaction of the final blends.[3,15–17]

One method of improving the interfacial interaction is to increase the polarity of PP. This is often done by grafting PP with a polar monomer such as maleic anhydride (MA) to form grafted PP.[18–20] PP has also been functionalized with acidic groups.[21–24] Successful commercial blends are then made by physically blending maleic or acidic functionalized PP at 5–10 wt % with the PP matrix. PP-*g*-MA has been used as an adhesion promoter, especially in composites.[25–27] This has been shown to improve the interfacial adhesion between the PP matrix and the filler through polar/polar interactions.

One approach to improving the miscibility is to functionalize the rubber and PP. This was successful using epoxidized NR, sulfonated EPDM, or a coupling agent such as *m*-phenylenebismaleimide in a maleated PP matrix.[28–30] Recent work done by Kim et al.[17] concluded that the addition of an ionomer such as poly(ethylene-*co*-methacrylic acid) ionomers and the application of dynamic vulcanization can improve the miscibility of PP and EPDM. It has been shown that ternary blends of a divalent ionomer, PP, and microgel EPDM show the behavior of a thermoplastic interpenetrating network, based on the rheological properties, crystallization behavior, and morphology. In addition, Jancar et al.[1] investigated a blend of maleated PP with EPR and maleated EPR with PP. They reported that the grafting of MA onto EPR did not change the elastomer modulus or its adhesion to PP, and the elongations at break for maleated PP/EPR blends were lower than those for nonmaleated PP-based blends.

A limitation of these approaches is that there is no chemical bonding between the PP and the rubber phase. To form chemical bonds between the phases, a third phase which has reactive groups that can be chemically bonded with the matrix and the rubber phase must be used. This has been found to improve the mechanical properties of the blends.[31] Therefore, this study focused on improving the interfacial adhesion of maleated PP/maleated EPDM blends. The interfacial adhesion was altered by the addition of a third reactive polymer, a polyetheramine (PEA, polyoxypropylenediamine) to chemically bond the EPDM and PP. The goals of this study were: 1) to investigate the effect of maleated EPDM rubber in maleated PP on the physical and mechanical properties; and 2) to maximize the toughness of the blend by improving the interfacial adhesion. The effects of the reactive polymer at several concentrations and its molecular weights on the morphology and mechanical properties of the PP/EPDM blends are presented and discussed.

EXPERIMENTAL

Table I summarizes several important characteristics of the materials used in this study. Table II lists the formulation of the blends studied. The PP-*g*-MA was dried overnight in an tray oven at 80°C to ensure the removal of residual moisture. All other polymers were used as received. The polymers, in pellet form, were dry-blended with the stabilizers. The liquid polyoxypropylenediamine was poured over the dried, premixed polymers and stirred to ensure uniform mixing. Reactive extrusion was carried out in a corotating intermeshing Leistritz LSM 34 GL twin-screw extruder (8 zone plus a die, L/D ~ 30) with a vacuum. The screw design was selected to ensure intensive and uniform mixing for an efficient reaction to take place in the extruder. The temperature for all zones was controlled at 200°C. The experiments were carried out at a screw speed of 275 rpm and a throughput of 30 lb/h. Pelletized resins were dried at 80°C overnight in an dehumidifying oven and molded in test specimens following ASTM D638.

FTIR was performed to identify the chemical reaction among the rubber, the PP matrix, and the compatibilizer using a Bio-Rad Win-IR spectrometer with a resolution of 4 cm^{-1}. Samples for FTIR analysis were in the form of thin films which were obtained by cutting a thin middle section of the injection-molded tensile bar. The films were then compressed at 230°C for 1 min into 1-mm-thick specimens, using a Carver press set at 1000 psi.

Optical microscopy was used to study the morphology of the blends. Samples were cut out from the injection-molded tensile bars, mounted in epoxy, and then polished using a LECO VP 160 polisher with 240, 400, 800, and 1000 grit paper followed by aluminum oxide powder at 1 and 0.06 μm. For better phase contrast and assessment of the particle sizes, the rubber was etched out from the PP matrix using methylene chloride at room temperature for a maximum of 1 min. Optical micrographs were taken perpendicular to the injection direction. SEM was used to view the fracture

Table I Material Characteristics

Materials	Trade Name	Sources	MFI	M_w	M_n	MA Content, (wt %)	Other Characteristics/ Comments
PP	KP010	Montell, Inc.	10 dg/min[a]	229,000	46,200		Xylene soluble 2.4%
Maleated PP	Epolene E-43	Eastman		9100	3900	3.7[b]	
Maleated EPDM	Royaltuf 465	Uniroyal Chem.	53[c]	400,000	150,000	~ 1.0	Ethylene/propylene = 55/45
Polyoxypropylenediamine	Jeffamine D-400	Hunstman	—	400	—	—	Primary amine = 4.3 meq/g
Polyoxypropylenediamine	Jeffamine D-2000	Hunstman	—	2000	—	—	Primary amine = 1 meq/g

[a] ASTM 1238 at 2160 g and 230°C.
[b] Calculated from acid no. 47.
[c] Mooney viscosity (ML = 1 + 4) at 125°C.

surface of tensile samples tested at room temperature. The samples were gold-coated and viewed with a Amray Model 1830/D4.

Dynamic and thermal properties were measured with a thermal dynamic analyzer Model DMTA Mark II. The midsection of the ASTM D638 tensile bars were cut for analysis. The specimen was run by cooling the sample in the Rheometrics temperature chamber to −100°C using liquid nitrogen and then heating at a constant heating rate of 3°C/min at a frequency of 1 Hz to at least 160°C, which is close to the melting temperature of PP. The bending mode was used. The glass transition temperature, T_g, loss peaks, tan δ, and elastic modulus, E', were measured as a function of temperature.

The onset crystallization temperature and heat of fusion were obtained on a Perkin–Elmer DSC series 7 at a heating rate of 10°C/min. The weight percent crystallinity for the blend was calculated by taking the ratio of the peak heat of fusion of the blend to that of the 100% crystalline PP which has a value of 208 J/g.

A Kayeness Galazy V capillary rheometer was used to measure the apparent viscosity as a function of shear rate in the range from 30 to 28,125/s and a constant processing temperature of 200°C. Melt flow data were obtained using a Tinius–Olsen melt indexer similar to a procedure described in ASTM D-1238. The test temperature was set at 230°C and the total weight was 2160 g. The extruded time was 1 min.

The mechanical properties were measured as follows: The Izod impact strength was measured using ASTM D-256 with a 2 lb_f pendulum. To provide uniform clamping pressure on all specimens, a torque wrench capable of 20–40 in. lbs was used to clamp the samples. The standard specimen was cut from the center section of the ASTM D638 injection-molded tensile bar. A specimen notching machine TMI Model 22-05-03 was used to create a V notch on the specimen. The cutter speed was set at 6 and the feed speed was set at 5. After notching, the width of the specimen at the tip of the notch was 0.400 ± 0.002 in. Each specimen was calibrated for the notch depth. See Figure 1 for details on notch dimensions.

The notched Izod impact strength was calculated as follows:

$$I_S = (E_S - E_{TC})/t$$

where I_S is the impact strength J/m of the width; t, the width of the specimen or the width of the

Table II Blend Formulations

Materials	M = Maleated Matrix	E-1	E-2	E-3	E-4	E-5
PP homopolymer	75	60	59	58.2	56.4	58.2
Maleated PP, PP-*g*-MA	25	20	19.7	19.4	18.8	19.4
Maleated EPDM, EPDM-*g*-MA		20	19.7	19.4	18.8	19.4
Polyoxypropylenediamine D-400		0	1.6	3	6	
Polyoxypropylenediamine D-2000						3
MA/NH_2 molar ratio			8.8/1	5/1	2.5/1	2.5/1

notch, m; E_S, the uncorrected breaking energy of specimen, J; and E_{TC}, the total energy correction for a given breaking energy, J.

The tensile properties were measured using ASTM D638-89 for tensile properties at a crosshead speed of 50 mm/min. The tensile modulus (Young's modulus) was calculated from the slope of the steepest line that occurs in the linear portion of the load/displacement curve. The computer used a least-squares linear regression to calculate this value.

The flexural modulus and strength were measured on an Instron, Model 4202-serial 1256. A 64-mm-long section was cut from the narrow center guage region of an injection-molded ASTM D638 type I tensile bar. This type of specimen is in accordance with ASTM D4101. A three-point bending test using a three-point flexural jig with a 51-mm-test span was used with a self-calibrating tension 200 lb (90.7 kg) load cell. The flex jig was set up to provide a three-point loading system per ASTM D790, method I, with a 9.525-mm-diameter anvil and support. The crosshead speed was set at 0.05 in/min (1.27 mm/min) and the specimens were deflected until a maximum strain of 5% if no rupture occurred. The flexural strength at 5%

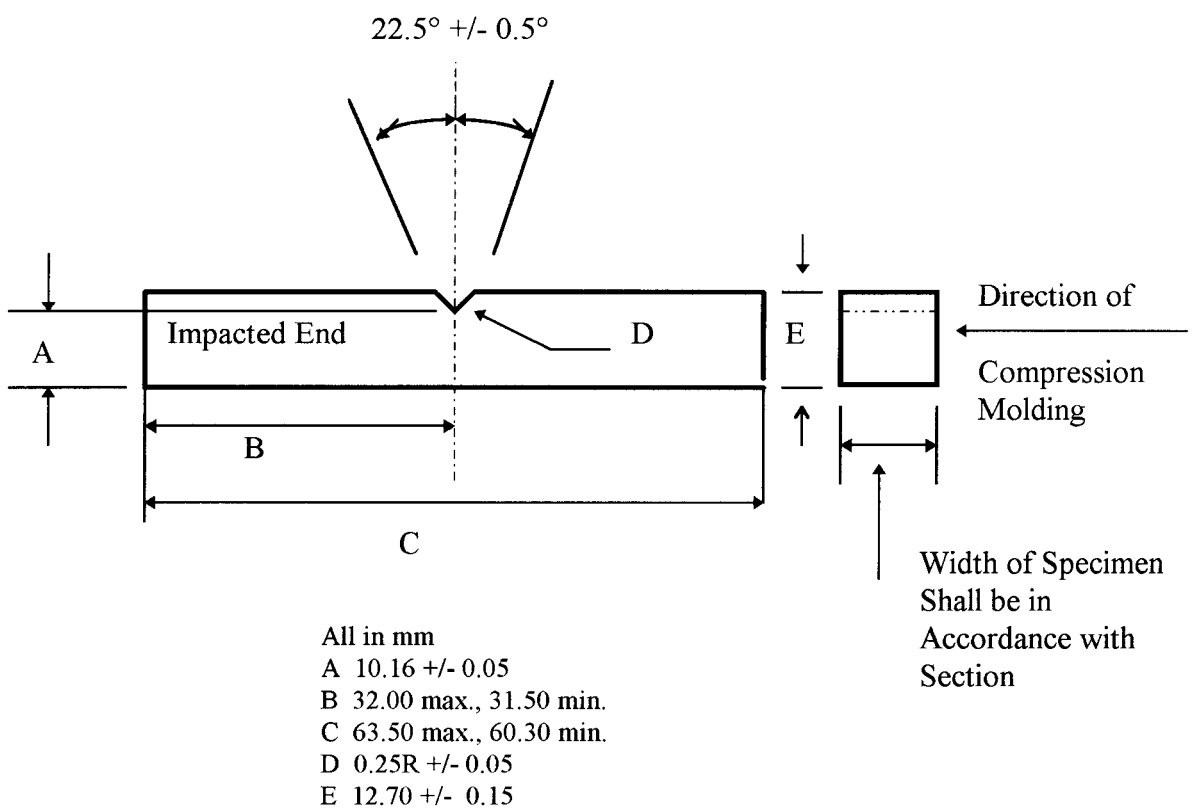

Figure 1 Dimension of Izod-type test specimen.

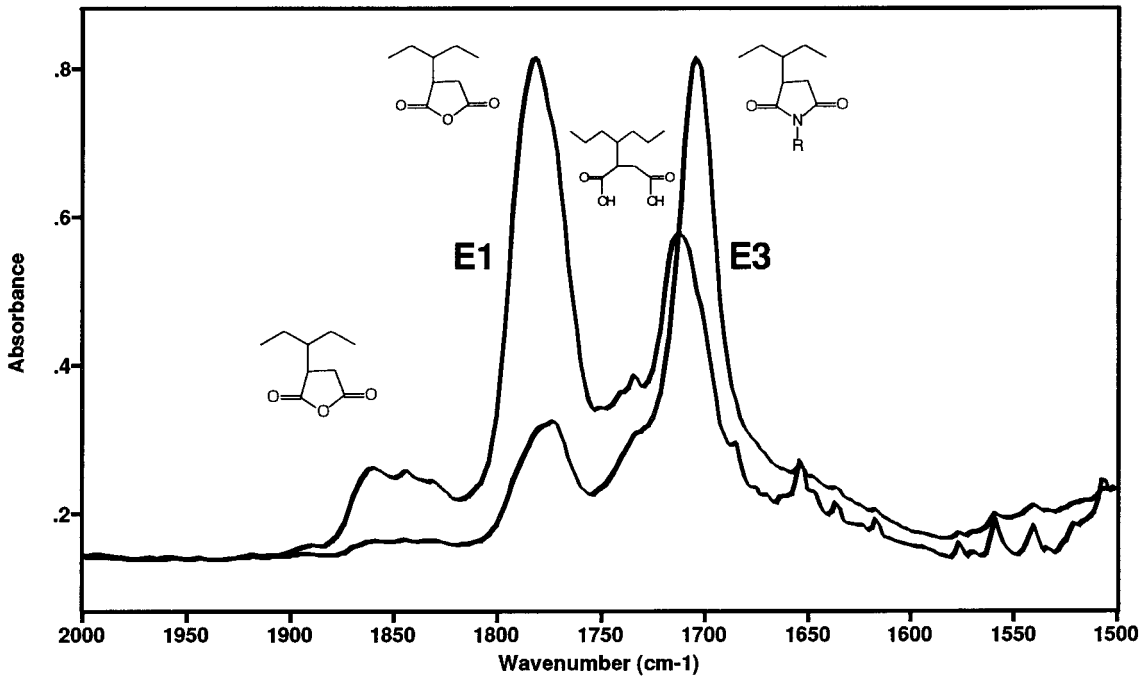

Figure 2 FTIR spectra of the C=O stretching in the region of 2000–1500 cm^{-1} wavenumber: (E1) 0% PEA; (E3) 3 wt % PEA.

strain and the flexural modulus at 1% secant are reported. The 1% secant modulus is defined as the slope of the line which is drawn on the stress versus strain curve that connects 0 and 1% strain.

RESULTS AND DISCUSSION

Compatibilization Mechanism and FTIR Analysis

Figure 2 shows the spectra of blends E-1 (0% PEA) and E-3 (3% PEA as a compatibilizer) for maleated EPDM and maleated PP blends. The area of interest is in the wavelength region from 2000 to 1500 cm^{-1}. Spectra E-1 shows peaks at 1859 and 1781 cm^{-1}. These peaks are the anhydride stretching of the MA in the PP and the EPDM rubber. In the E-3 blend which contains 3 wt % PEA, there are significant reductions in the absorbances of the MA peaks at 1859 and 1781 cm^{-1}. This indicates that a reaction of MA and the amines indeed occurs. There is also some unreacted MA; this is expected because the molar ratio between MA/NH_2 for blend E3 is about 5/1. In addition, there are two strong peaks which appear at approximately 1703 and 1774 cm^{-1} in the E-3 blend. These peaks correspond to the C=O stretches of the imide structure,[32] indicating that imide linkages form. Amide (**A**) is the intermediate of the reaction. The IR spectra, however, show no detection of N—H or O—H stretches at 3300–3500 cm^{-1} or amide carbonyl stretch at 1650 cm^{-1} or carboxylic acid stretch at 1713 cm^{-1}. This indicates that as soon as amide was formed it underwent ring cyclization to yield imide (**B**).

Spectra of blend E-1 also show a strong peak at 1713 cm^{-1}. This is identified as the C=O stretch corresponding to the dicarboxylic acid (**C**). This could be due to the ring-opening reaction between the MA with moisture. This reaction can occur during the film preparation for FTIR analysis. However, there is no acid peak in the spectra of the blend with PEA (E-3). Table III summarizes the positions of the peaks as identified from the spectra.

Figure 3 summarizes all the possible mechanisms that occur during the melt reactive blending of maleated PP, maleated EPDM, and PEA. The amine functionalities in PEA react with the MA moieties in PP and EPDM to form imide linkages. The imide linkage can be formed between the PP/PP chains (B1), between PP and the rubber chains (B2), and between the rubber/rubber chains (B3). All three competitive reactions presumably occur simultaneously during the short residence time in the extruder, but the kinetics of

Table III Summary of Positions of the C=O Stretches of Compounds Found in Maleated PP/Maleated EPDM/Polyoxypropylenediamine Blends

Compound	Chemical Structure of Species	Position (cm^{-1})	Comments
Maleic anhydride	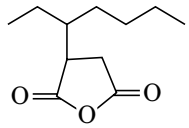	1860 and 1781	Unreacted MA (of the maleated PP) gives rise to absorption bands in the same region that grafted MA
Amide (**A**)	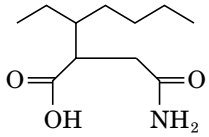	1670 for amide, 1713 for carboxylic	No detection on either C=O stretches at these wavelengths indicates all amide converts to imide
Imide (**B1, B2,** or **B3**)	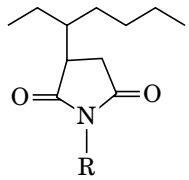	1703 and 1774	The presence of these peaks indicates the formation of imide
Carboxylic acid (**C**)	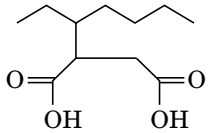	1713	Detection only in blend without PEA; possible reaction of MA and moisture

each reaction is not known. In our opinion, the formation of the imide linkage depends strongly on 1) the diffusivity of reactants which relates to the molecular weight and the mobility of all involved reactants at the reaction temperature of 200°C and 2) the concentration and distribution of the MA along the PP and the rubber chains.

The high concentration of MA in the matrix and the low molecular weights of both PEA and PP-*g*-MA are believed to be the driving force for the faster formation of B1 and B2 compared to B3. The PEA can easily access the MA groups on the PP backbone due the low molecular weight of the PP-*g*-MA and PEA compared to the relatively high molecular weight of the rubber, 4×10^5. Thus, the reaction between the PP-*g*-MA macromolecules with the PEA (to give B1) is more likely compared to the reaction between the PEA and the rubbers (to give B3). In addition, the MA content in the matrix is three times higher than that of the rubber (total MA 3.7 versus 1%, respectively). If the MA groups on the PP and the rubber chains are approximate within the vicinity of the PEA, then crosslinking between PP and the rubber via the imide linkage will also occur (to give B2). The formation of B2 is more likely than is B3 because of the low molecular weight and thus short chain length of the PEA macromolecules (M_w = 400) and the PP compared to the rubber and because of the higher MA concentration in the maleated PP matrix. The formation of B2 where one backbone is the PP and the other is the rubber is the desirable reaction in which PP and the rubber are chemically bonded via the imide linkage.

The formation of both B1 and B2 affects the mechanical properties of the PP matrix but to different degrees. The effect of PEA in blends of PP/PP-*g*-MA (where the imide formation is exclusively B1) has been reported.[33] It was shown in this patent that there is a slight improvement in the impact strength from 9 to 20 J/m with 4% PEA and 20% of PP-*g*-MA in the blend (with PP). As demonstrated in this study, however, the formation of B2 is believed to have a more significant effect on the mechanical properties, especially in improving the toughness. The formation of B3 is likely to have a negative toughening effect. If the rubber crosslinks, it will not uniformly disperse in the matrix.

The FTIR confirmed the formation of imide when the PEA reacted with the MA functionality in the PP matrix and the rubber. However, it is difficult to quantify the extent of the formation of

each species, B1, B2, and B3, because it only shows the imide linkage as a whole. Perhaps an investigation on the kinetic and fractionation method to access the formation of these compounds may be useful for further understanding the role of each on the toughening effect. However, this is beyond the scope of this investigation.

Effects of the Compatibilizer on Morphology

Figure 4(a–d) shows optical micrographs of maleated EPDM/maleated PP blends at 0, 1.6, 3, and 6 wt % of PEA, respectively. The effect of the compatibilizer (PEA) on the morphology of the blends is demonstrated in these pictures. The PP matrix appears as the white background. The holes (as dark gray to black) indicate that the discrete-phase EPDM in the blend has been dissolved into methylene chloride during etching. PEA will not be present as a separate phase because of its low molecular weight.

For the blend without the compatibilizer, the rubber phase formed particles of uneven size but similar geometry. The particle size is in the range from 2 to 5 μm. The blend with 1.6 wt % PEA shows a finer dispersion of rubber particles and a reduction in particle size by more than a factor of two. Most of the particles are in the size of 0.5 μm, with the exception of a few larger particles in the range up to 5 μm. As the PEA level increases to 3 wt %, qualitatively, there appears to be a broader distribution of rubber particle sizes compared to the blend with 1.6 wt % PEA. However, most of the particles remain relatively small compared to the blend without PEA, approximately from 1 to 5 μm, and some are still as small as about 0.5 μm. At 6 wt % PEA, there are some rubber particles of irregular shape, called "chunks," on the order of 10 μm or larger.

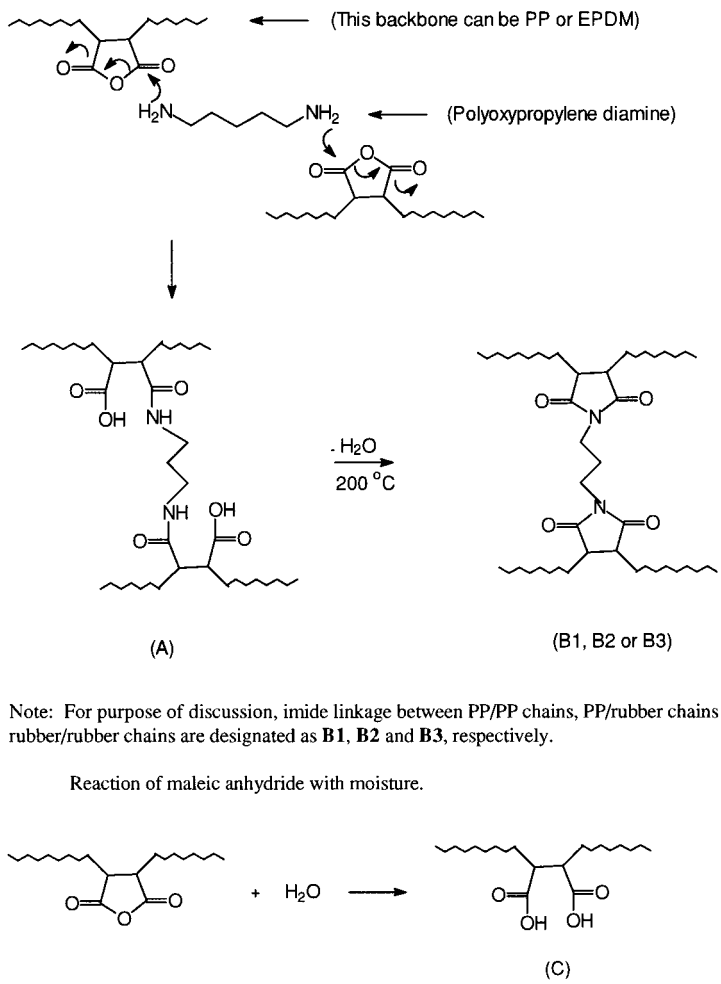

Figure 3 Ring-opening reaction mechanism of MA and polyoxypropylenediamine.

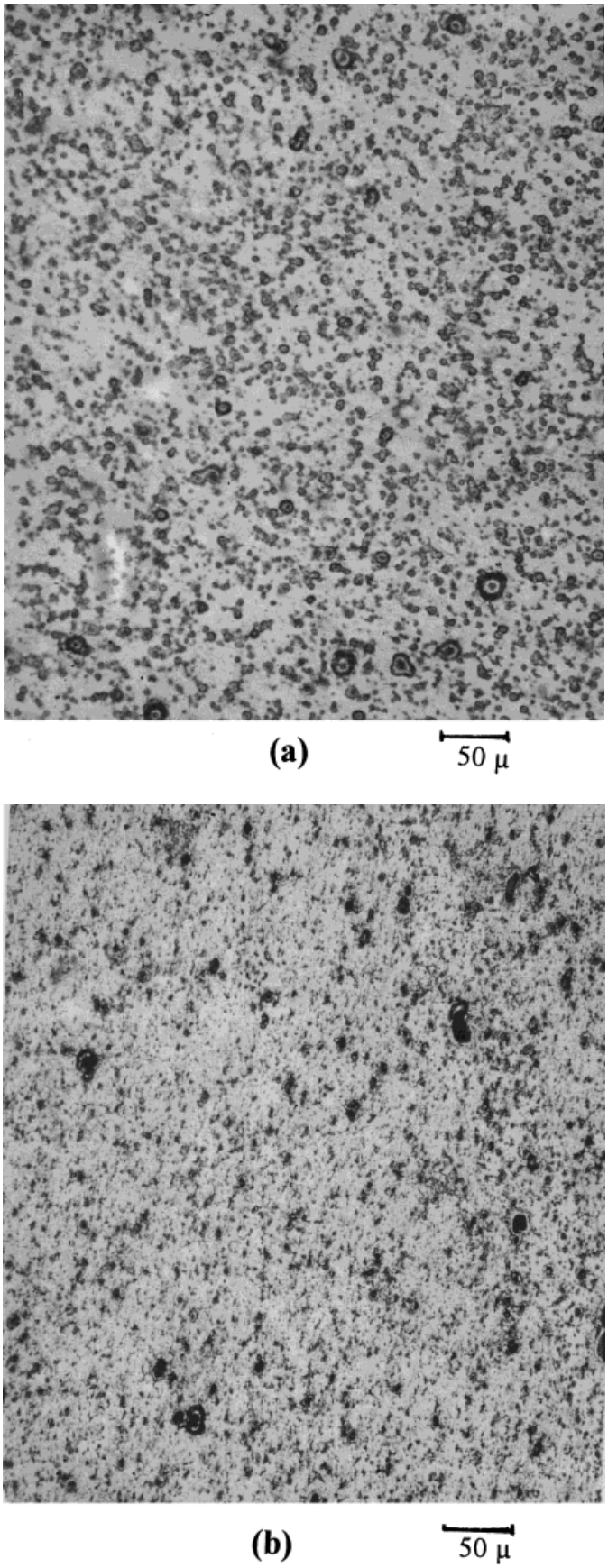

Figure 4 Optical micrographs at 200× of PP/maleated EPDM blends at various levels of PEA: (a) 0, (b) 1.6, (c) 3, and (d) 6 wt %.

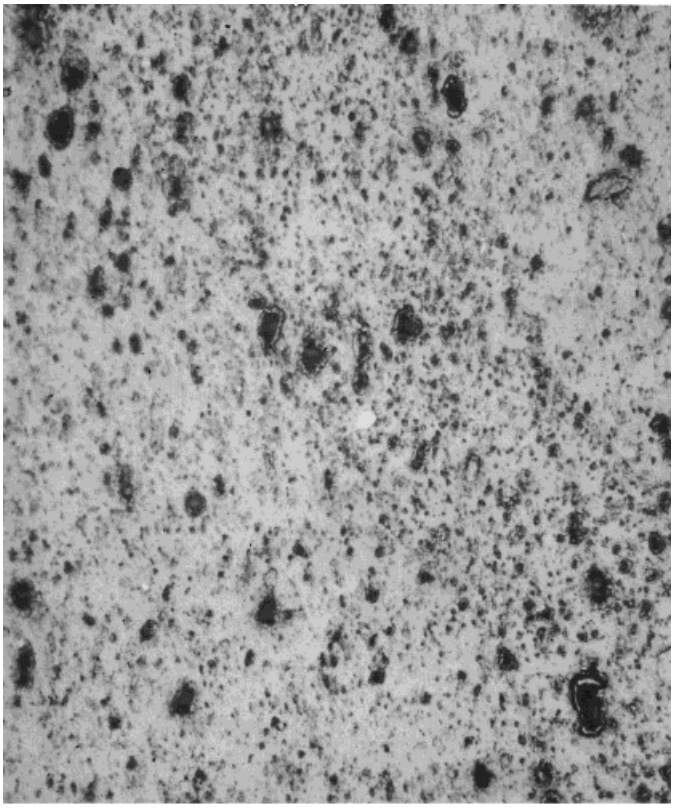

(c) 50 μ

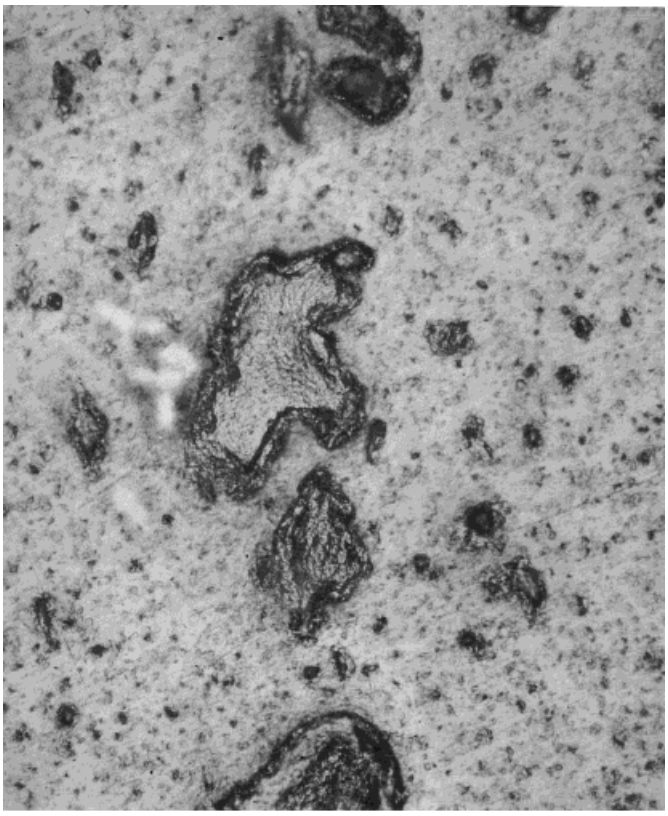

(d) 50 μ

Figure 4 (*Continued from the previous page*)

These "chunks" contain smaller particles inside them.

The effect of PEA as a compatibilizer is clearly demonstrated by the micrographs of the blends. It is important to note that the "chunks" that appeared in Figure 4(c,d) for maleated EPDM blends with 3 and 6 wt % PEA, respectively, were not totally removed from the matrix (no dark holes) during methylene chloride etching. This suggests that these "chunks" are gels or microgels which might be formed by the crosslinking of either B1 or B3, but not B2, and are not soluble in methylene chloride. The increase in the size of these chunks with increasing PEA content indicates that more crosslinking has taken place because more PEA is available for reaction. The "chunk" enlargement at a high level of PEA may also be due to the agglomeration of these microgels as a result of more crosslinking.

Figures 5 and 6 show SEM micrographs of the tensile fracture surface of the maleated EPDM/maleated PP blend at 0 and 3 wt % PEA. In blends with 3 wt % PEA, the rubber cavitated from the matrix during fracture instead of pulling cleanly out of the matrix, although it is apparent that the fracture is a brittle fracture for both blends. This suggests that the higher toughness in the 3 wt % blend is the result of an increase in interfacial bonding between the matrix and the rubber in the presence of PEA. The bonding between the rubber and matrix via the imide linkage, as confirmed by the FTIR analysis, is responsible for the improvement in the interfacial bonding compared to the blends without PEA where the PP and the rubber interaction is purely physical.

Effect of the Compatibilizer on Dynamic Mechanical and Thermal Properties

Dynamic mechanical testing provides a method for determining the elastic and loss moduli as a function of temperature. This provides information on the compatibility, the degree of polymer crystallinity, and stiffness of the polymer, and it is useful as a relative comparison of the dynamic behavior of different blends.

The damping capacities (dynamic moduli E') and the tan δ of PP and maleated PP as a function of temperature are essentially the same as shown in Figure 7, which indicates that the blend of PP/PP-*g*-MA may be thermodynamically miscible. The peak of tan δ, however, is slightly higher for the maleated PP, especially just above the T_g of the PP at approximately 19°C. There is also another transition at 75°C. This is probably associated with the crystalline structure of the isotatic PP. Figure 8 shows the Log(tan δ) and Log(E') for maleated EPDM. The maleated EPDM shows a glass transition temperature at about −29.5°C. Figure 9 shows Log(tan δ) as a function of temperature for the maleated EPDM, the maleated PP matrix, a blend without the PEA compatibilizer, and a blend with 3 wt % PEA. Two main relaxation regions are observed: The transition around −30°C is the glass transition of the maleated EPDM. The relaxation region around 19°C is the glass transition of PP. The positions of both peaks were not changed by the blending with maleated EPDM. Thus, there is no significant interaction between maleated PP and maleated EPDM. As can be seen in Figure 9, maleated EPDM has a considerably higher damping capacity than has maleated PP, resulting in lower damping capacities for the blends relative to pure maleated EPDM.

The change in the peak height of tan δ in the temperature region between −100 and 50°C for blends at various levels of PEA for maleated EPDM is shown in Figures 9 and 10. There is a clear trend in the variation in tan δ. The relative magnitudes of these loss peaks increase with increasing PEA content, and tan δ is highest for the 3 wt % PEA. In addition, the peak positions (for the elastomeric and the matrix) shift toward each other, and the shift appears to be more pronounced as the PEA concentration increases from 3 to 6 wt %. This indicates that there is partial miscibility in the system when PEA is used as a compatibilizer. The increase in the magnitude of the tan δ for blends using PEA as a compatibilizer suggests that there is an increase in the volume fraction of the amorphous region in the PP. This makes sense because the increase in crosslinking that was found using FTIR will make it more difficult for the polymer to crystallize. This conclusion is supported by the DSC measurements. As shown in Table IV, the addition of 20 wt % of the elastomer (maleated EPDM) to the maleated PP matrix reduced the weight percent of the crystallinity (weight percent crystalline PP in the total blend) from 49.4 to 39.2 wt % as expected. The weight percent of crystalline PP further decreased from 39.2 to 35%, and the onset of the crystallization peak temperatures increased from 116.7 to 118.7°C as the PEA concentration increased from 0 to 6 wt %. Notice that the onset of the crystallization peak temperature is the highest for the blend with 3 wt % PEA, 119.3°C.

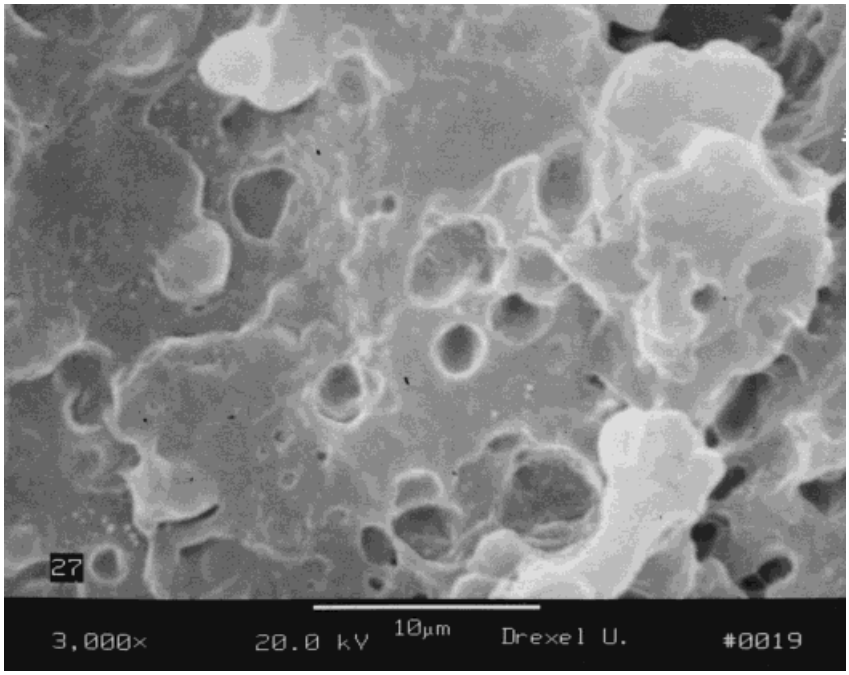

Figure 5 SEM micrograph of the tensile fracture surface at room temperature of a PP/maleated PP/maleated EPDM/PEA at 60/20/20/0 wt %.

Various types of correlation between the impact strength and dynamic mechanical properties have been presented in the literature,[9,34] such as (i) the occurrence of the peaks of the impact strength at the same temperature as the loss peaks in tan δ, (ii) linear variations of the impact strength with tan δ and an in-phase modulus, and/or (iii) correlation between the impact

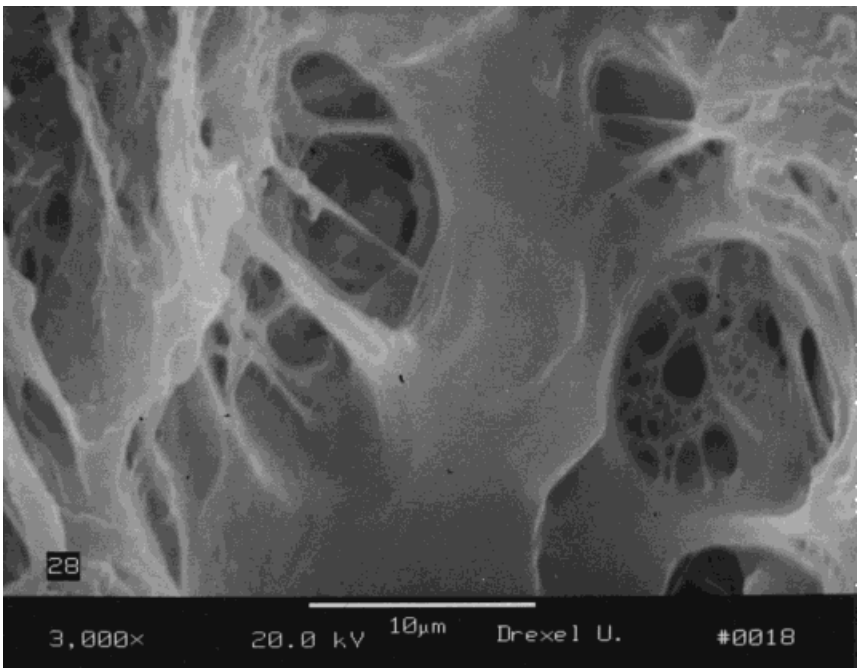

Figure 6 SEM micrograph of the tensile fracture surface at room temperature of a PP/maleated PP/maleated EPDM/PEA at 58.2/19.4/19.4/3 wt %.

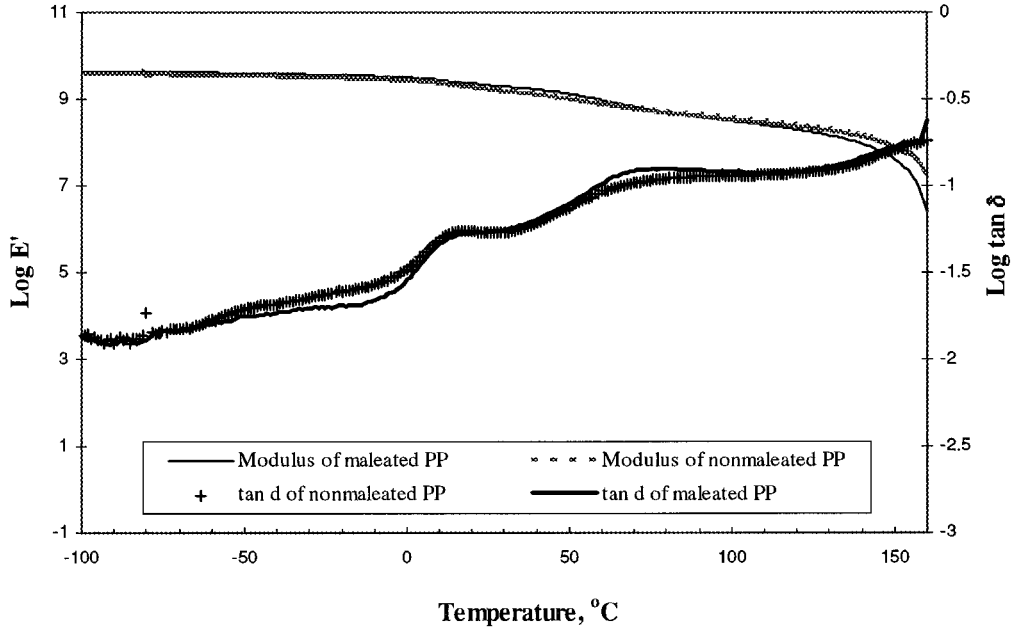

Figure 7 Tan δ and elastic modulus E' (-100 to 150°C) of maleated PP matrix (PP/PP-*g*-MA blend at 75/25 wt %) and nonmaleated PP matrix (100% PP).

strength and area of the rubber component's loss peak, and/or (iv) correlation of the impact strength at a given temperature with the area under the dynamic mechanical loss peaks, for both the areas of the matrix and the elastomeric component's loss peaks. In blends of SEBS/PP, Gupta and Purwar[9] found a correlation between the area under the dynamic mechanical loss peaks and the impact strength at a given test temperature. It was concluded that at ambient temperature toughening is predominantly due to shear yielding plus the viscoelastic energy dissipation of relaxation of both the PP matrix and the elastomer, whereas at -30°C, the toughening is predominantly due to crazing and viscoelastic energy dissipation of the elastomer component's relax-

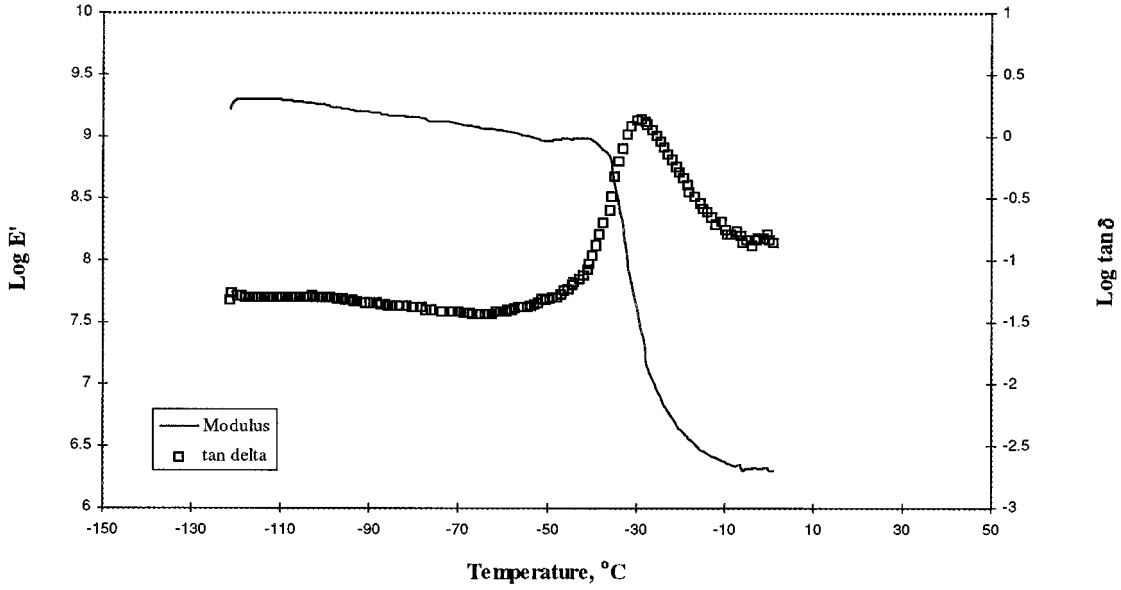

Figure 8 Tan δ and elastic modulus E' (-150 to 50°C) of maleated EPDM.

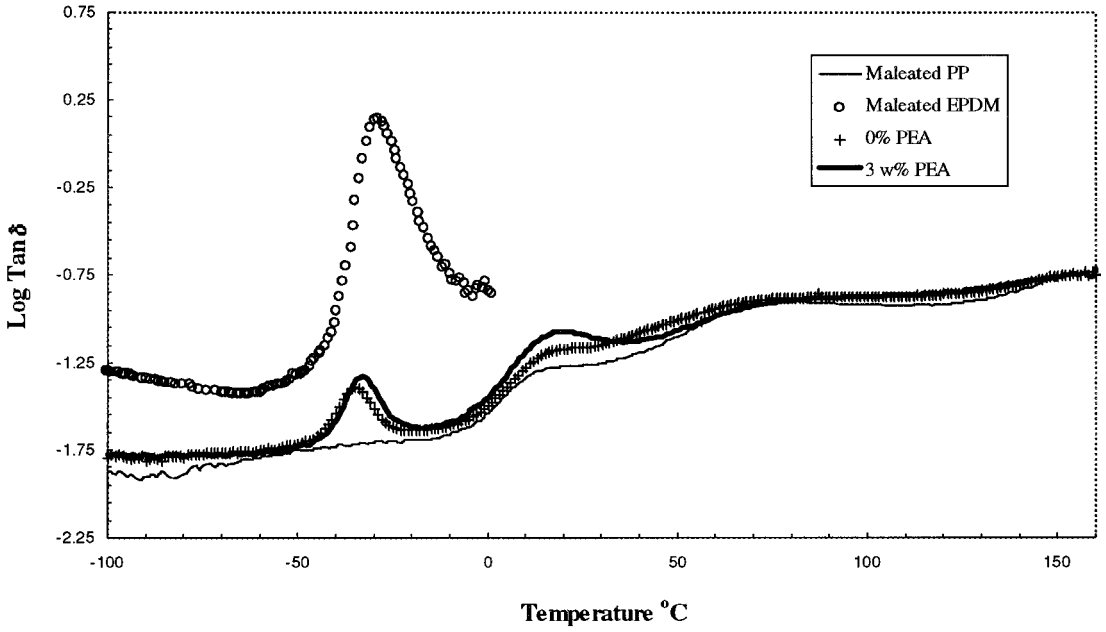

Figure 9 Comparison of the tan δ (-100 to 150°C) maleated EPDM, maleated PP matrix, and their blends with 0 and 3 wt % PEA.

ation. In our study, blends of maleated EPDM/maleated PP show that the rubber component's loss peak which is smaller in area does not vary much with PEA concentration. However, the area of the dynamic mechanical loss peaks of the PP matrix increased as the PEA concentration increased. This suggested that there is a higher viscoelastic energy dissipation associated with the blends using the PEA compatibilizer. It will be shown in the Mechanical Properties section that, indeed, the increase in the area of the dynamic mechanical loss peaks of the PP matrix corresponds to the increase in the impact strength.

There is also an effect of the PEA molecular weight on the magnitude of tan δ and the relative peak positions at 3 wt % of PEA. Figure 11 shows tan δ as a function of temperature for the maleated EPDM blend at 3 wt % PEA but for two dif-

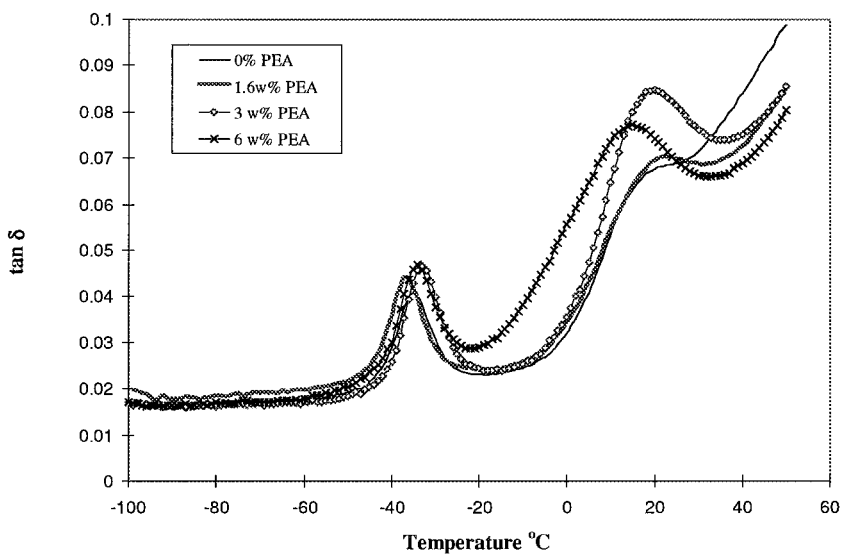

Figure 10 Comparison of the tan δ (-100 to 50°C) linear scale for maleated EPDM/maleated PP blends at various levels of PEA: 0, 1.6, 3, and 6 wt %.

Table IV Heat of Fusion and Weight Percent Crystallinity at Various Levels and Molecular Weights of PEA

Weight Percent PEA	Heat of Fusion (J/g)	Onset Crystallization Temp (°C)	% Crystallinity
Maleated PP matrix[a]	102.7	116.9	49.4
0	81.5	116.7	39.2
1.6	79.6	117.8	38.2
3	76.9	119.3	37.0
6	72.9	118.7	35.0
3[b]	78.6	119.1	37.8

[a] Maleated PP matrix (PP/PP-*g*-MA blend at 75/25 wt %).
[b] Polyoxypropylenediamine at a molecular weight of 2000. All other blends used PEA with a molecular weight of 400.

ferent molecular weights of PEA. The tan δ of the blend using lower molecular weight PEA (E-3) is higher than that of the blend using higher molecular weight PEA (E-5). The difference in the magnitude of the tan δ peaks is more significant near the T_g of PP. The shift in the tan δ peaks (both the elastomeric and the matrix) toward each other is also more pronounced when lower molecular weight PEA was used. This indicates that better compatibility or enhanced miscibility was obtained. The larger dynamic mechanical loss peak associated with blends using lower molecular weight PEA indicates a higher amorphous volume in these blends. However, the DSC results did not support this conclusion. As shown in Table IV, the weight percent crystallinity is only marginally increased from 37 to 37.8% when PEA of higher molecular weight was used and the onset of crystallization is similar at 119°C. The only explanation we have is that there is also another unknown transition peak in the tan δ curve of the high molecular weight PEA blend at approximately −10°C. This transition peak does not appear in any blend with low molecular weight PEA (Figs. 10 and 11). This transition may be due to a distinct amorphous phase in these blends and would explain why the tan δ peak height at about 20°C is different even though the weight percent crystallinity is the same.

The reason that the low molecular weight PEA is more effective in compatibilizing the blend than is the high molecular weight PEA is that diffusion is more inhibited by the larger PEA molecules. The low molecular weight PEA has higher chain mobility which reacts more easily with the MA functionality on the PP and the rubber. Furthermore, there are more chain ends and higher amine functional groups associated with the lower molecular weight PEA (4.4 versus 1 meq/g of total amine). Consequently,

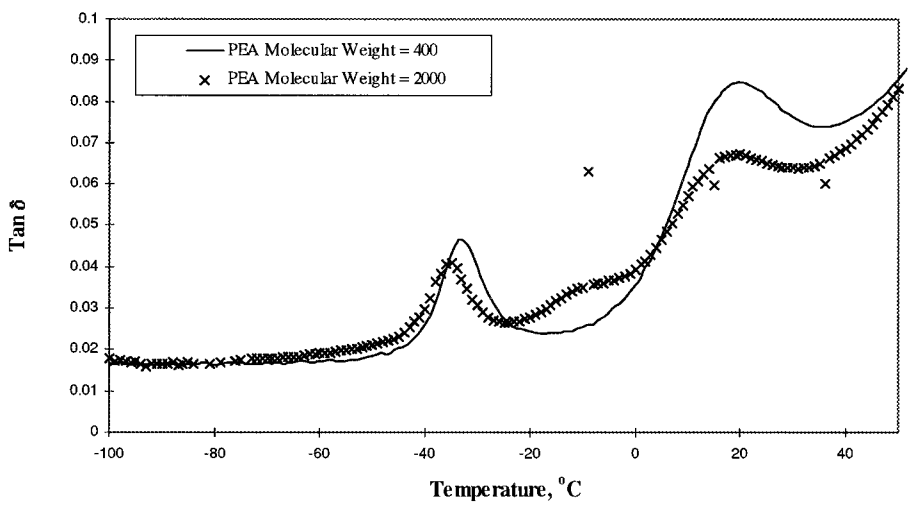

Figure 11 Comparison of the tan δ (−100 to 50°C) linear scale for maleated EPDM/maleated PP blends at a fixed level of PEA 3 wt %, but two different molecular weights.

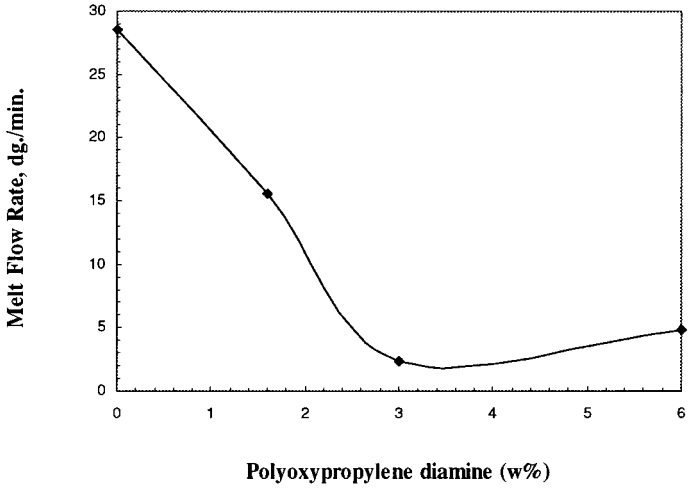

Figure 12 Melt flow rates of maleated EPDM/maleated PP blends as a function of polyoxypropylenediamine composition.

there are more imide linkages between the rubber and the matrix when low molecular weight PEA was used as a compatibilizer. In addition, when shorter-chain PEA was used, a shorter interfacial distance resulted which allowed more interdiffusion or more intimate contact of the rubber and the PP macromolecules. Thus, increasing the PEA molecular weight resulted in less crosslinking and fewer *in situ* chemical bonds between the rubber and the PP matrix. It will be shown that this has an impact on the mechanical properties of the blends.

Effect of the Compatibilizer on Rheological Properties

The addition of the PEA as a compatibilizer resulted in a significant reduction in the melt flow rate and increase in the apparent viscosity of the blend as shown in Figures 12–14. This reconfirms the FTIR, DMTA, and DSC data showing that crosslinking takes place when PEA is used as a compatibilizer. As a reference, it is of interest to observe the viscosity change with shear rate for nonmaleated PP, the maleated PP matrix, maleated rubbers, and their blends, as shown in Figure 13. It is clear that the maleated EPDM has a much higher viscosity compared to the PP matrix. It is also important to note that the maleated PP matrix has much lower viscosity compared to the nonmaleated PP. This is expected when the high viscosity nonmaleated PP matrix (M_w = 2.3 $\times 10^5$, MFI = 10 dg/min) is substituted with 25% by weight of the low molecular weight maleated PP (M_w = 9.1 $\times 10^3$, MFI > 100 dg/min). The maleated PP/maleated rubber blends have a viscosity in the range between that of the matrix and the maleated EPDM, as expected. Increasing the PEA level up to 3 wt % does not vary the viscosity of the blends much. It is apparent that the low shear viscosity increased slightly; however, the high shear viscosity differs only marginally as the PEA level increases in contrast to a drastic change in the melt flow rate from above 30 to ~ 2 dg/min. The trends, however, between the MFR and viscosity are in agreement (decrease in MFR, increase in viscosity). The relative increase in the viscosity as a function of PEA indicates that crosslinking occurred.

The molecular weight of the PEA compatibilizer also had an effect on the rheological properties of the blends. At the same level of PEA, a higher viscosity was obtained for blends using lower molecular weight PEA as shown in Figure 15. This can be explained because more crosslinking occurred in blends with lower molecular weight PEA. Although the melt flow rate is a quick guide to the melt processability, it corresponds to the viscosity of a single shear rate, which is generally low. Rubber-toughened PP is generally processed at a high shear rate and high shear viscosity. From our data which show that the viscosity is affected less as the shear rate increases, it is not expected that the addition of PEA will affect the processing parameters significantly.

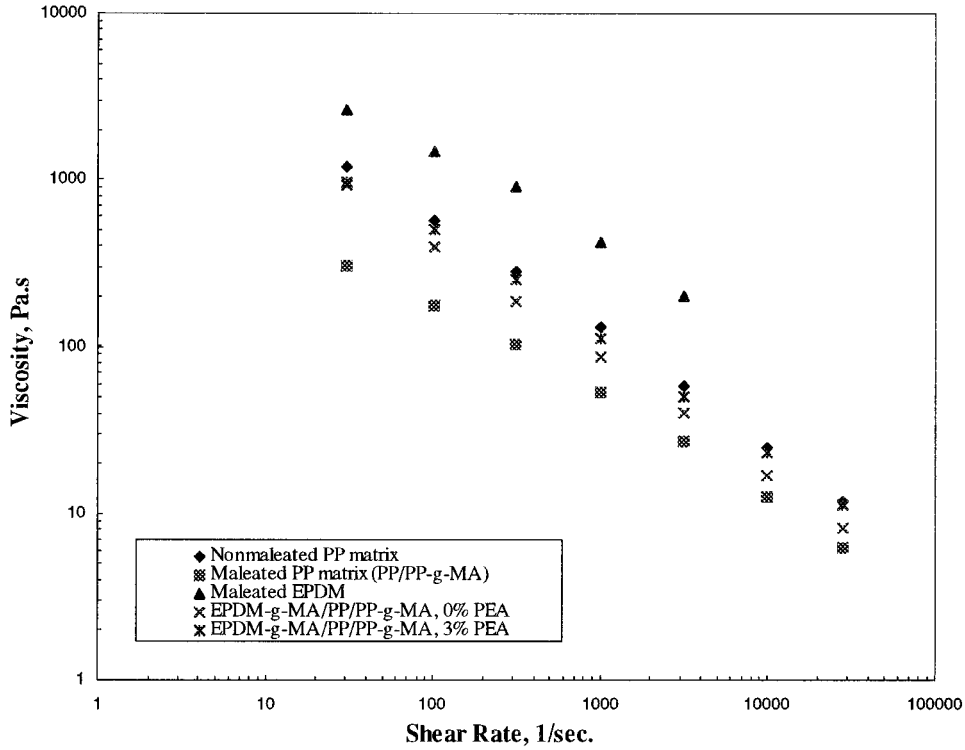

Figure 13 Viscosity of nonmaleated PP, maleated PP matrix, EPDM-*g*-MA, and EPDM-*g*-MA/PP/PP-*g*-MA blends with 0 and 3 wt % PEA as a function of shear rate and constant temperature at 200°C.

Effect of the Compatibilizer on Mechanical Properties

The morphology, rheological, and interface properties of polymer/rubber blends strongly influence their mechanical properties. The mechanisms affecting mechanical behavior fall into three general categories: enhancement of shear yielding, control of craze growth, and the rubber particles acting as defects:

1. Shear yielding can be enhanced because the rubber particles act as stress concentrators. This reduces the far-field stress required for local flow of the matrix. Therefore, rubber particles are expected to reduce the yield stress and increase the dissipative ability of the matrix (increase toughness). This effect is enhanced by weak interfacial adhesion in which the rubber particles are essentially holes. In addition, the size and dispersion of the rubber particles has been shown to be important. Jancar et al.[1] showed that there is an optimal interparticle spacing, and for EPDM-modified PP, the optimum average diameter appears to be approximately 0.4 μm.[5,35]
2. If there is strong interfacial adhesion between the rubber and the PP, then the rubber particle can control craze growth.[4] The rubber particles can span the craze and prevent further craze opening. This prevents the craze from becoming a crack.
3. Rubber particles, because of their small size, are also defects. They initiate failure as discussed above and, if large enough, can decrease the strength and toughness of the blend by creating a critical flaw size.

This study will be discussed in light of these three mechanisms.

The effect of PEA on the impact strength and stress–strain behavior is clearly demonstrated in Figures 16 and 17. The addition of maleated EPDM increased the impact strength of the maleated PP matrix from 10 to 44 J/m. The addition of the PEA compatibilizer further increased the impact strength of the blends from 44 to 120 J/m at PEA of 3 wt % as indicated by the Izod impact test and the increased area under the stress–strain curves. However, further increasing PEA to 6 wt % reduced the impact strength. In all the

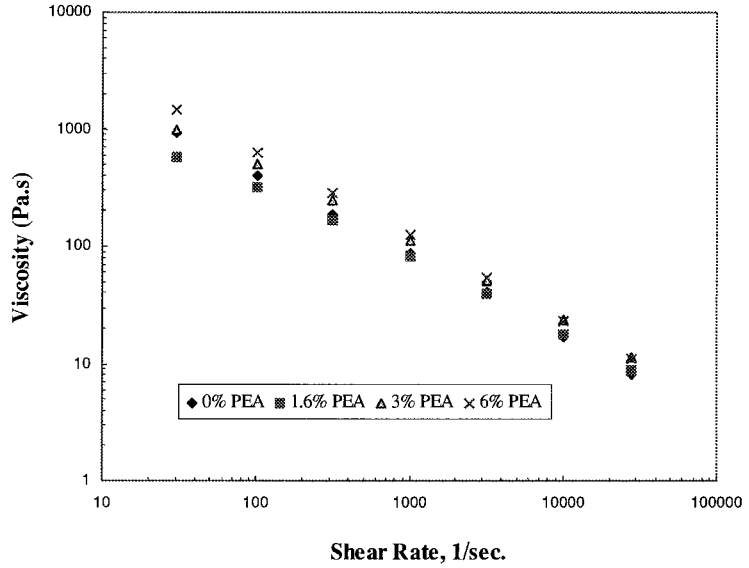

Figure 14 Viscosity of maleated EPDM/maleated PP blends as a function of shear rate and at different polyoxypropylenediamine compositions.

samples studied, stress-whitening was observed before the general yielding point, and such a whitening phenomenon continued to intensify in the unnecked zone even after cold drawing started. Because the stress whitening was not observed in the PP homopolymer, this indicates that it is most

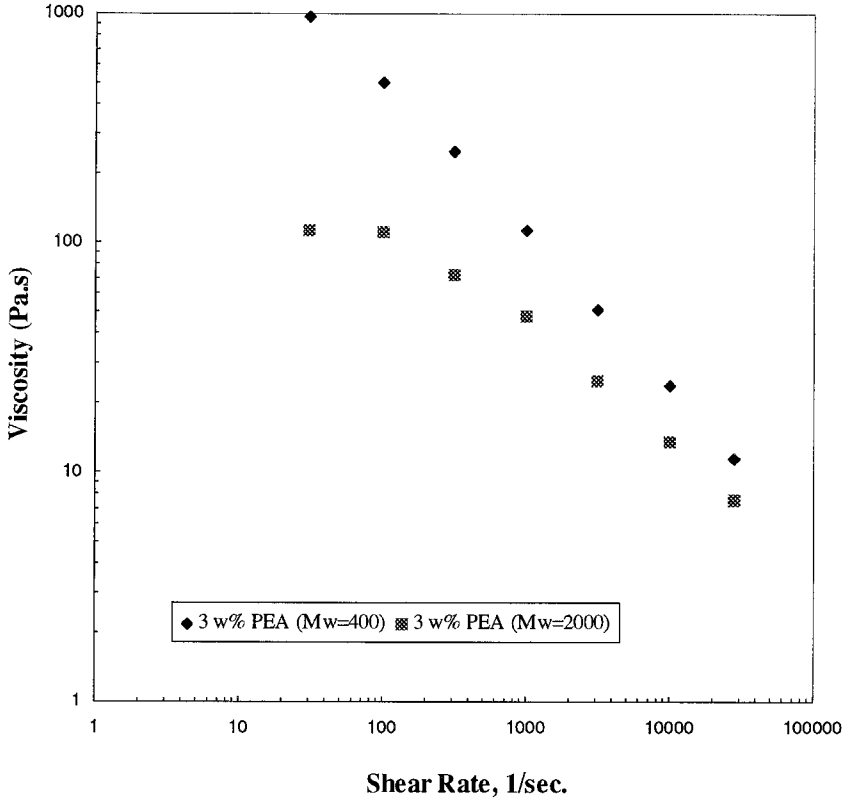

Figure 15 Viscosity of maleated EPDM/maleated PP blends as a function of shear rate and different polyoxypropylenediamine molecular weights.

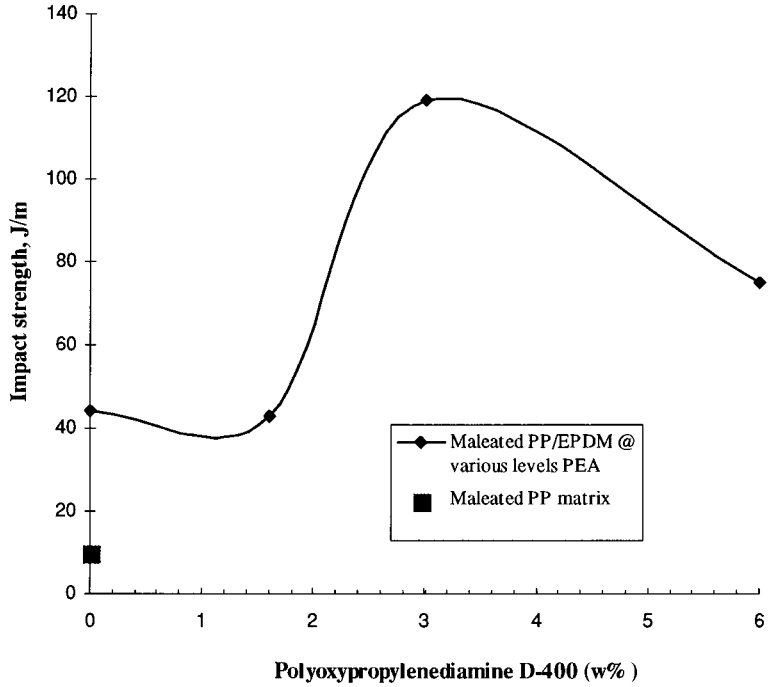

Figure 16 Impact strength for maleated EPDM blends as a function of polyoxypropylenediamine composition.

likely due to the formation of crazes and/or shear bands promoted by the rubbery phase in the modified systems.[1,4]

With 0% PEA, the rubber particles are poorly adhered to the matrix as shown by voids and dewetting of the particles on the fracture surfaces (Fig. 5). In this case, the only role of the rubber particles was as stress concentrators. This decreased the far-field stress at which the matrix began to flow and thus increased the volume of the plastic zone in front of the crack tip. The increased plastic zone increased the energy absorbed by the matrix and increased the toughness over that of maleated PP matrix as shown in Figures 16 and 17. The addition of PEA led to more interfacial adhesion (as proved via DMTA and microscopy, Figs. 5 and 6). The increased interfacial adhesion of the EPDM to the PP did two things: First, it decreased the average particle size, which according to Jancar[1] increases further the shear

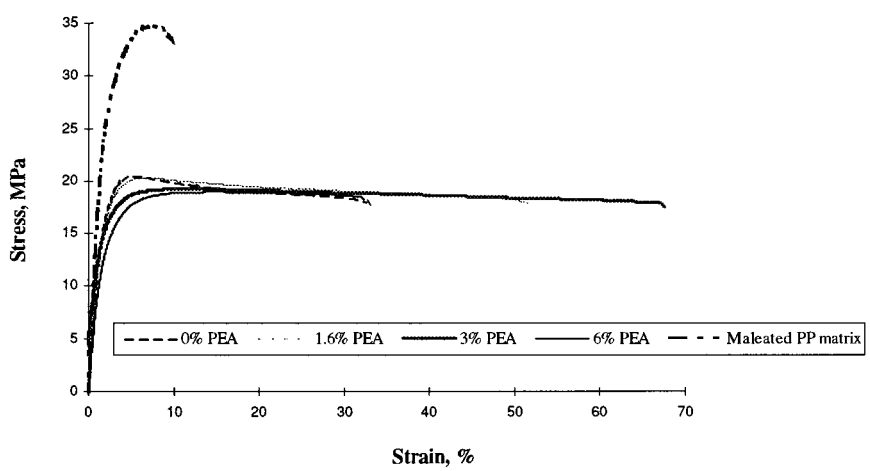

Figure 17 Stress–strain behavior of the maleated EPDM blends at various polyoxypropylenediamine compositions.

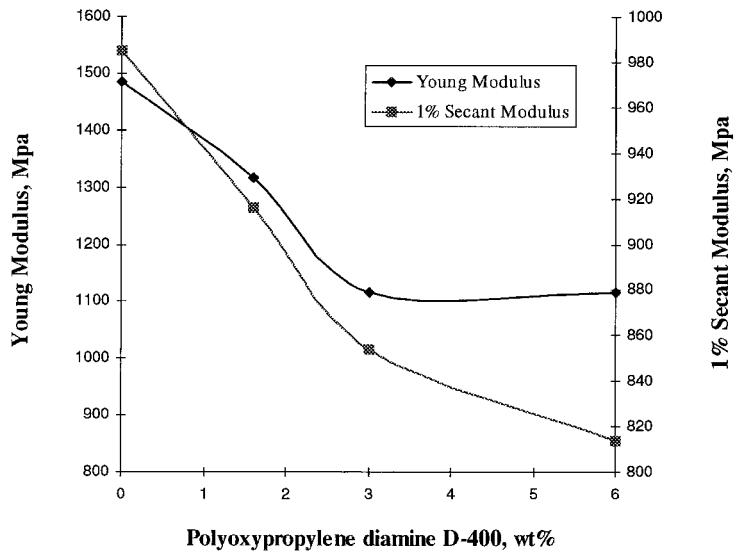

Figure 18 Young's modulus and secant modulus for maleated EPDM/maleated PP blends as a function of polyoxypropylenediamine composition.

yielding in the matrix. Second, the adhesion is reported to allow the rubber particles to span a craze and thus control crack growth within the craze.[36] This again increases the ability of the matrix to absorb energy. In addition, during fracture, the particles were cavitated rather than totally dewetted from the matrix and, hence, improved the impact resistance by absorbing energy.

The reduction in the impact strength at 6 wt % PEA can be explained by the presence of larger particles which act as defects. These defects led to an increase in the number of crack initiation sites and the magnitude of the stress field around the particles. Thus, the crack tends to initiate and to accelerate rapidly and reach a catastrophic size faster than does the blend with smaller and more regular particles. This process outweighs the plastic deformation of the rubber, thus leading to a reduction in fracture toughness. This is supported by the decrease in the elongation at fracture.

The tensile modulus and flexural modulus for all blends decreased as the PEA levels increased and then leveled off when the PEA was above 3 wt % (Fig. 18). The reduction in stiffness as a function of PEA is probably due to the presence of the crosslinking between the rubbery phase and

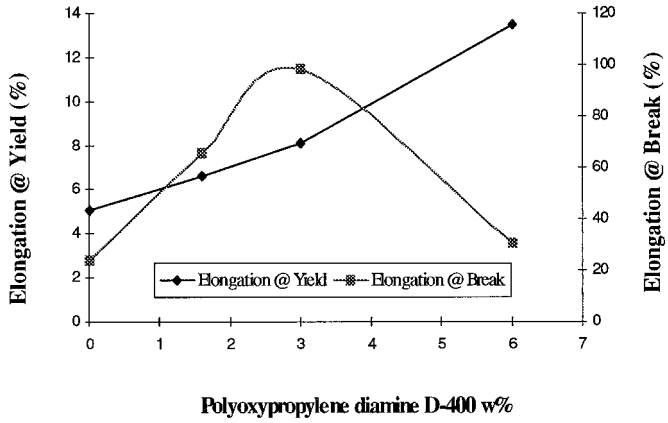

Figure 19 Elongation at yield and break for maleated EPDM/maleated PP blends as a function of polyoxypropylenediamine composition.

Table V Comparison of Mechanical Properties of Blends with Different PEA Molecular Weights

Materials	Composition (wt %) E = Blends of EPDM Rubber Type	
	E-3	E-5
PP homopolymer	58.2	58.2
Maleated PP, PP-*g*-MA	19.4	19.4
Maleated EPDM, EPDM-*g*-MA	19.4	19.4
Polyoxypropylenediamine D-400	3.0	
Polyoxypropylenediamine D-2000		3.0
Mechanical Properties at Ambient Temperature		
Notched Izod impact (J/m)	119.0	38.0
SD	9.0	3.0
Tensile strength at yield (Mpa)	19.2	19.1
SD	0.12	0.03
Tensile strength at weld line (Mpa)	17.2	17.1
SD	0.03	0.18
Weld line retension (%)	90.0	90.0
Tensile (Young's) modulus (Mpa)	1116.0	1372.0
SD	76.0	43.0
Elongation at yield (%)	8.12	6.07
SD	0.08	0.2
Elongation at break (%)	98.4	54.73
SD	2.0	4.0
Flexural strength at 5% strain (Mpa)	25.6	26.6
SD	0.1	0.2
Flexural modulus, 1% secant (Mpa)	854.0	944.0
SD	10.3	11.7

the matrix phase. As the crosslinking increases (higher PEA level), the weight percent of the PP crystalline phase is reduced as confirmed by the DSC and DMTA data. Therefore, the tensile and flexural modulus of the blend depends on the counterbalance of an increase in crosslinking and a decrease in crystallinity. Thus, in the presence of PEA, the decrease in crystallinity outweighs the increase in crosslinking.

The reduction in yield stress, strength, and flexural strength can be explained as follows: Because the rubber particles act as stress concentrators, they decrease the far-field stress at which the matrix will begin to flow. This decreases the macroscopic yield stress. In addition, as the level of PEA increased, the particles decreased in size. This has been shown to further decrease the far-field stress at which local plastic flow will occur.

The elongation at yield and elongation at break were found to be optimum when the PEA level was 3 wt % (Fig. 19). These properties are strongly influenced by the degree of interfacial adhesion between the rubber and the matrix. The improvement in these properties are obviously a result of increasing the interfacial adhesion as revealed by the morphology of the blends. The improved adhesion between the EPDM/PP interface helped to reduce the role of the rubber as defects. The reduction at 6 wt % is again probably due to the "chunks" becoming so large that the low modulus of the rubber again made it a failure initiation site.

The molecular weight of the PEA compatibilizer also had a significant effect on the mechanical properties of the blends as shown in Table V. Lower molecular weight PEA ($M_w = 400$) gave better impact strength, higher elongation at break and yield, and similar tensile strength. However, higher molecular weight PEA ($M_w = 2000$) gave a slightly higher tensile and flexural modulus. Nevertheless, the overall mechanical property balance is more de-

sirable for blends using low molecular weight PEA. The better impact strength and ductility can be explained from the DMTA and rheological data. Again, the increase in the tan δ, the inward shift of the peak positions as revealed by DMTA, and the reduction in the viscosity of the blend using lower molecular weight PEA conveys a higher degree of crosslinking between the matrix and the rubber, thus better compatibility and, consequently, more improvement in the mechanical properties.

In summary, the improvement in the impact resistance, elongation at break, and yield in maleated EPDM/maleated PP blends correlated well with the rheology, DMTA, and morphology. The role of the polyoxypropylenediamine is clearly defined as the compatibilizer for the maleated EPDM/maleated PP blends in which it modified the interfacial properties of the immiscible blends, leading to an increase in the interfacial adhesion and, consequently, improvement in many mechanical properties.

CONCLUSIONS

1. The polyxolypropylenediamine acts as a reactive polymeric compatibilizer in the blend of maleated EPDM/maleated PP blends. It modified the interfacial properties of the immiscible blends, leading to an increase in the interfacial adhesion.
2. The compatibilization is a result of the formations of imide linkage *in situ* between the rubber and the matrix.
3. The maximum toughness is achieved with increasing interfacial adhesion and possibly broadening of the particle sizes.
4. The reduction in the modulus and tensile strength was a result of a counterbalance between the increase in the crosslinking and decrease in crystallinity.
5. The optimum concentration of compatibilizer is found to be 3 wt %, and this corresponds to a $\frac{1}{5}$ NH_2/MA molar ratio.
6. Blends of maleated PP/maleated EPDM are immiscible but compatible, and their compatibility was further improved with PEA as a compatibilizer.

The authors wish to acknowledge Mr. David J. Von Rohr of Drexel University for his assistance in obtaining many of the fine micrographs. Dr. Riad Gobran at Drexel University is also acknowledged for his comments and fruitful discussion. One of the authors (T.P.) is grateful to Montell Polyolefins for financially supporting this work.

REFERENCES

1. J. Jancar, A. DiAnselmo, A. T. DiBenedetto, and J. Kucera, *Polymer,* **34,** 1684 (1993).
2. F. C. Stehling, T. Huff, S. Speed, and G. Wissler, *J. Appl. Polym. Sci.,* **26,** 2693 (1981).
3. P. Galli, S. Danesi, and T. Simonazzi, *Polym. Eng. Sci.,* **24,** 544 (1984).
4. B. Z. Jang, D. R. Uhlmann, and J. B. Vander Sande, *J. Appl. Polym. Sci.,* **30,** 2485 (1985).
5. B. Z. Jang, D. R. Uhlmann, and J. B. Vander Sande, *J. Polym. Eng. Sci.,* **25,** 643 (1985).
6. L. D'Orazio, C. Mancarella, E. Martuscelli, and F. Polato, *Polymer,* **32,** 1186 (1991).
7. L. D'Orazio, C. Mancarella, E. Martuscelli, G. Sticotti, and P. Massari, *Polymer,* **34,** 3671 (1993).
8. B. Pukanszky, I. Fortelny, J. Kovar, and F. Tudos, *Plast. Rubb. Comp. Proc. Appl.,* **15,** 31 (1991).
9. A. K. Gupta and S. N. Purwar, *J. Appl. Polym. Sci.,* **29,** 3513 (1984).
10. A. K. Gupta and S. N. Purwar, *J. Appl. Polym. Sci.,* **31,** 535 (1986).
11. J. Karger-Kocsis, A. Kallo, A. Szafner, G. Bodor, and Z. Senyer, *Polymer,* **20,** 37 (1979).
12. A. J. Tinker, *Polym. Commun.,* **25,** 325 (1984).
13. L. K. Yoon, C. H. Choi, and B. K. Kim, *J. Appl. Polym. Sci.,* **56,** 239 (1995).
14. E. N. Kresge, *J. Appl. Polym. Sci. Appl. Polym. Symp.,* **39,** 37 (1984).
15. D. Yang, B. Zhang, Y. Yang, Z. Fang, G. Sun, and Z. Feng, *Polym. Eng. Sci.,* **24,** 612 (1984).
16. C. S. Ha and S. C. Kim, *J. Appl. Polym. Sci.,* **37,** 317 (1989).
17. Y. Kim, W. J. Cho, C. S. Ha, and W. Kim, *J. Polym. Eng. Sci.,* **35,** 1592 (1995).
18. D. E. Reid and H. M. Spurlin, U.S. Patent 3,414,551, 1968.
19. R. Rengarajan, V. R. Parameswaran, S. Lee, and P. L. Rinaldi, *Polymer,* **31,** 1703 (1990).
20. B. De Roover, M. Sclavons, V. Carlier, J. Devaus, R. Legras, and A. Momtaz, *J. Polym. Sci. Part A Polym. Chem.,* **33,** 829 (1995).
21. M. Xanthos and S. S. Dagli, *Polym. Eng. Sci.,* **31,** 929 (1991).
22. X. Li and D. Wang, *Chin. J. Polym. Sci.,* **10,** 328 (1992).
23. H. S. Moon, B. K. Ryoo, and J. K. Park, *J. Polym. Sci. Polym. Phys. Ed.,* **32,** 1427 (1994).
24. J. Y. Wu et al., *Adv. Polym. Tech.,* **14,** 47 (1995).
25. E. Fontan, O. Laguna, and E. P. Collar, *J. Polym. Mater.,* **7,** 139 (1990).
26. J. Taranco, O. Laguna, and E. P. Collar, *J. Polym. Eng.,* **11,** 325 (1992).

27. J. Jancar and A. T. DiBenedetto, *Macromolecules,* **25,** 399 (1992).
28. N. R. Choulhury and A. K. Bhowmick, *J. Appl. Polym. Sci.,* **38,** 1091 (1989).
29. N. M. Mathew and A. J. Tinker, *J. Nat. Rubb. Res.,* **1,** 240 (1986).
30. S. Norzalia, H. Hanim, and M. Y. Ahmad Fuad, *J. Plast. Rubb. Compos. Process. Appl.,* **22,** 185 (1994).
31. K. Chanramouli and S. A. Jabarin, *J. Adv. Polym. Tech.,* **14,** 35 (1995).
32. I. M. Vermeesch, G. Groeninckx, and M. M. Coleman, *Macromolecules,* **26,** 6643 (1993).
33. R. K. Evans, R. J. G. Dominguez, and R. J. Clark, Eur. Pat. Appl.: Huntsman Corporation, Publication number 0 634 424 A1, 1994.
34. J. Karger-Kocsis and V. N. Kuleznev, *Polymer,* **23,** 699 (1982).
35. M. T. Gallaghter, *ANTEC'91,* 2389 (1991).
36. C. B. Bucknall, *Toughened Plastics,* Applied Science, London, 1977.